UNCLASSIFIED

AD NUMBER

AD307724

CLASSIFICATION CHANGES

TO: unclassified

FROM: secret

LIMITATION CHANGES

TO:

Approved for public release, distribution unlimited

FROM:

Distribution authorized to DoD only; Operational and administrative use; 31 Dec 1957. Other requests shall be referred to Diamond Ordnance Fuze Lab., Washington, 25, DC.

AUTHORITY

HDL, D/A ltr, 15 Aug 1979; HDL, D/A ltr, 15 aug 1979

THIS PAGE IS UNCLASSIFIED

SECRET

AD 307724

Armed Services Technical Information Agency

ARLINGTON HALL STATION
ARLINGTON 12 VIRGINIA

FOR

MICRO-CARD

CONTROL ONLY

SECRET

THEORETICAL ANALYSIS
OF A DASH-DOT SENSING SYSTEM (U)

31 December 1957

by

Orval R. Cruzan

Orval R. Cruzan

SECRET

DIAMOND ORDNANCE FUZE LABORATORIES
ORDNANCE CORPS   WASHINGTON 25, D. C.

THEORETICAL ANALYSIS
OF A DASH-DOT SENSING SYSTEM (U)

TA3-5205	31 December 1957	TR-433
DA504-07-002		53 Pages
DOFL Proj. 52850	by	Copy No. __

Orval R. Cruzan
Orval R. Cruzan

FOR THE COMMANDER:

Approved by
J H Van Trump for
H. P. Kalmus
Chief, Laboratory 50

SECRET

SECRET

TABLE OF CONTENTS

SECRET

SECRET

TABLE OF CONTENTS (continued)

SECRET

ABSTRACT (S)

A theoretical analysis is made of a Dash-Dot Sensing System containing photosensitive elements. For such a system to be highly effective the trajectory of a target missile must be known with a considerable degree of accuracy. Several methods for determining the trajectory are analyzed. Special cases of these methods are used to obtain simple formulas, to be solved by an electronic computer, for the firing-time T_f and the firing-position Y_f of shaped-charges, the jets of which render the target nonlethal. An error analysis is made, which, in effect, extends the analysis from an ideal to an actual sensing system. Resolving ability of the system is discussed. Various arrangements of the system to provide special protective features are considered.

1. INTRODUCTION

For the automatic defense of armored fortifications, vehicles, and vessels, such as bunkers, tanks, landing craft, etc., of which the armor provided is not sufficient to resist the lethal power of a range of target missiles, a Dash-Dot Sensing System has been proposed. Throughout the report, when the word "target" is used it will refer to the missile that is to be intercepted. In general, this system consists of an arrangement of photosensitive elements or photo-detectors and shaped-charges together with an electronic computer. Regarding the activation of the detectors, the system may be active or passive as suits the intended use. The active system is one in which the regions observed by the detectors are illuminated by light sources contained within the system. In the passive system, the illumination is provided by external sources, e.g., the sun, atmospheric scattering of sunlight, luminous targets, etc.

To indicate the purpose of each part of the system, it is desirable to consider the system in operation. The target is assumed to be traversing a rectilinear trajectory at uniform speed. The times of passage of a sequence of detectors and the positions of these detectors are observed. This information is transmitted to an electronic computer. The computer calculates the shaped-charge firing-time T_f and firing-position Y_f, so that the shaped-charge jet can render the target nonlethal.

The primary purpose of this report is to obtain formulas for the firing-time T_f and the firing-position Y_f of a shaped-charge in forms which can be quickly solved by an electronic computer. A second purpose is to determine the simplest arrangement of detectors that will provide the necessary and sufficient information required by the computer. A third purpose is to give groupings of these simple arrangements which will provide special protective features. Experimental work on the

Dash-Dot Sensing System involving results obtained in this report,
has been reported by L. Melamed, H. W. Straub, R. R. Ulrich in
DOFL Report TR-470, "A Sensing System for Dash-Dot," 1 Sept 1957.

In this theoretical report, following a description of the
general detector and shaped-charge arrangements, and the operation
of the system, a mathematical analysis is made, deriving the shaped-
charge firing-time T_f and the firing-position Y_f. Next an analysis
is given for special cases of the system. Following this an error
analysis is made of the special cases which, in effect, amounts to
an extension of the analysis of an ideal system to an actual one.
Next a short digression is made concerning the resolving ability of
the system with respect to several missiles. Finally various
groupings of the system to provide special protective features, such
as defense of corners, walls and surfaces; defense of the detectors
and the shaped-charges; and etc., are considered.

2. DESCRIPTION OF ARMAMENT AND DETECTOR OF A DASH-DOT SENSING SYSTEM

To assist in describing the armament and the detectors of a Dash-Dot Sensing System, which may be used for the defense of fortifications, vehicles,and vessels, e.g., bunkers, tanks, landing-craft, etc., consider a schematic of such illustrated in Figure 1. Assume that a side of the armored device is represented by the wall W. Making an angle θ with the wall is a flat imaginary surface S; the value of the angle θ is arbitrary or may depend on a special arrangement of the system as considered in section 6. The armament consists of a row of equally spaced shaped-charges, in a straight line, OY, situated in the surface S. The row which may be attached to out-riggers, not shown in Figure 1, is in general, parallel to the wall W and may be some distance b from it. The length of the row will depend upon the amount of protection required; in many cases, it may extend from one end of the wall to the other or beyond. The axes of the shaped-charges in a row are parallel to each other and make an angle ψ_4 with a normal $\hat{n}_4$. This normal lies in a plane determined by the axes of the shaped-charges and is perpendicular to the straight line OY, that is formed by the row. The plane, as thus determined, is referred to as the shaped-charge or β-fence, and it makes an angle β with a normal to the surface S.

Attached to out-riggers (not shown in Figure 1) are several rows in the surface S of equally spaced photosensitive detectors. These rows are parallel to that of the shaped-charges. In general, there need be, at most, only four rows of detectors located at various distances from the shaped-charges. The distance of the row farthest from the shaped-charges is designated as s_0; the distance of the next or second farthest as s_1; for the third row, s_2; and the distance of the fourth and nearest row as s_3. Each detector is so designed that it views a restricted region of space, e.g., a cylindrical region coaxial with the axis of the detector. As with the armament, the axes of the detectors in each row are parallel to each other and make an angle ψ_n with a normal $\hat{n}_n$. These normals lie in planes determined by the axes of the detectors and are perpendicular to the straight lines which are formed by the rows. In the first row $\psi_n = \psi_0$; in the second row, $\psi_n = \psi_1$; etc. In general, the ψ's have different values; restrictions on their values are derived in section 3, which is devoted to the mathematical analysis. The planes determined by the detector axes are referred to as the detector fences, and they make various angles α_n with the normal $\hat{n}$ to the surface S.

With respect to light sources, the system may be passive or active. In the passive system, the illumination, the interception of which gives rise to electrical impulses by the detectors, is provided by sources external to the system, such as sunlight, luminous missiles, etc. For the active system, the illumination is provided by the system. The illumination is obtained from the most suitable arrangement. This may
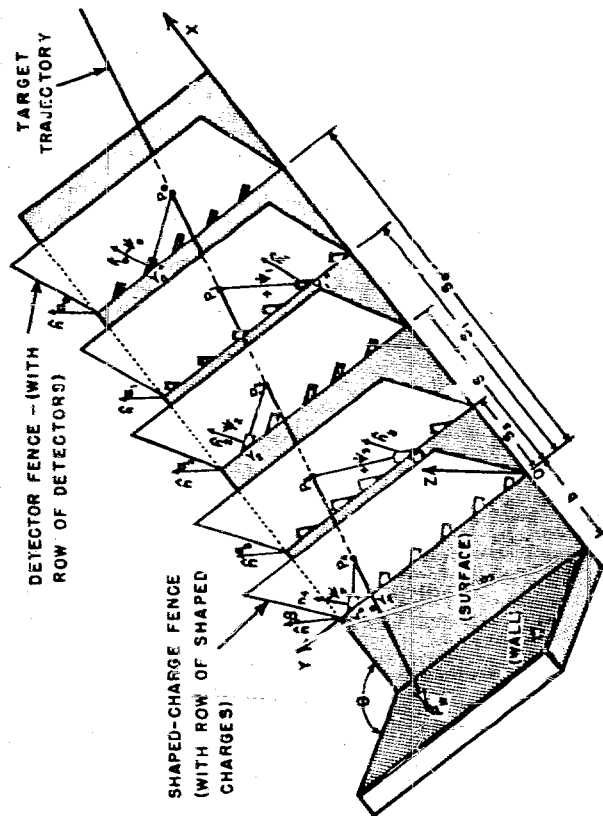
Figure 1. General Arrangement of Armament and Detectors of Dash-Dot Sensing System.

be flood-lighting of the regions observed by the detectors, by strip-lighting to illuminate only individual rows of the observed regions, or by illuminating the individual detector observation regions by light sources concomitant with the detectors.

When operating, the system detects in succession the passage of the different detector fences by a target approaching the point P_w of the wall V. The time of activation and the position of the detectors activated in each fence are fed to a computer. As shown in the various figures, the trajectory of the target is intersected by the lines of observation of the detectors in the different rows. In actuality, this is an ideal, but possibly, rare situation. But for theoretical purposes it will be assumed that whenever the target crosses a detector fence, its longitudinal position in the fence is known, just as if a detector had been in the correct position to observe the passage. The fact that a detector is not correctly situated is considered in section 4. Upon receiving the information from the detectors the computer predicts the firing-time T_f and the firing-position Y_f of the appropriate shaped-charges. Thus when the target crosses the shaped-charge fence β, it is intercepted by high-velocity metal jets from the appropriate shaped-charges. This interception renders the target nonlethal to the armored device.

In the analysis of the Dash-Dot Sensing System, it is shown that under certain conditions, the system reduces to certain special cases. Three of these cases are schematically illustrated in Figures 2a, 2b, and 2c. The first of these cases, Figure 2a, arises from assuming that all target trajectories are parallel to the surface S, that $\psi_0 = \psi_1 = \psi_2 = \psi_4 = 0$, and that $\alpha_0 = \alpha_2 = \beta$. Under these assumptions, the α_3-fence is not needed. For the second case, Figure 2b, all similar angles are made numerically equal, that is, $\psi = \psi_0 = -\psi_1 = \psi_2 = -\psi_3$, $\psi_4 = \pm\psi$, and $\alpha_0 = \alpha_1 = \alpha_2 = \alpha_3 = \beta$. Under these conditions s_0 can be made equal to s_1, and s_2 made equal to s_3. With the third case, Figure 2c, ψ_4 is taken equal to zero, while all the other angles remain the same as in the second case. In the second and third cases, the detectors, instead of consisting of two separate rows in each fence, can now be made to consist of one row, but with each detector observing in the two directions $+\psi$ and $-\psi$.

$\psi = \psi_0 = \psi_1 = \psi_2 = \psi_4 = 0$

$a = a_0 = a_2 = \beta$

a_3 - FENCE NOT NEEDED
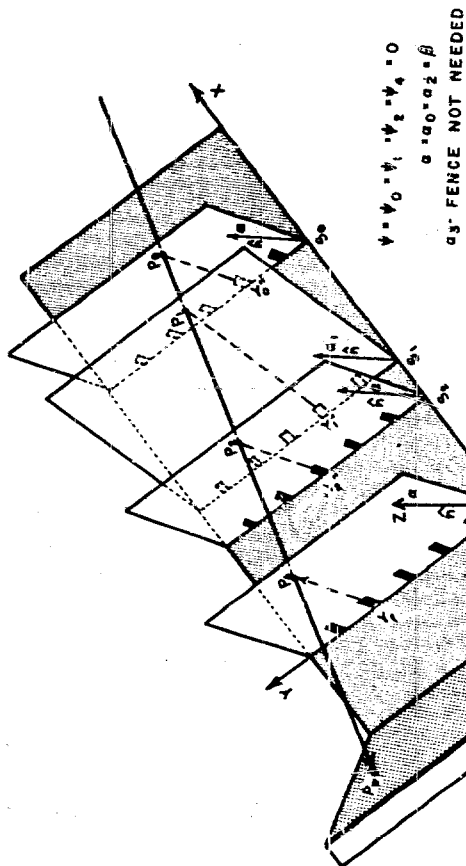
Figure 2a. Special Case of Dash-Dot Sensing System (Trajectory Parallel to S).

10
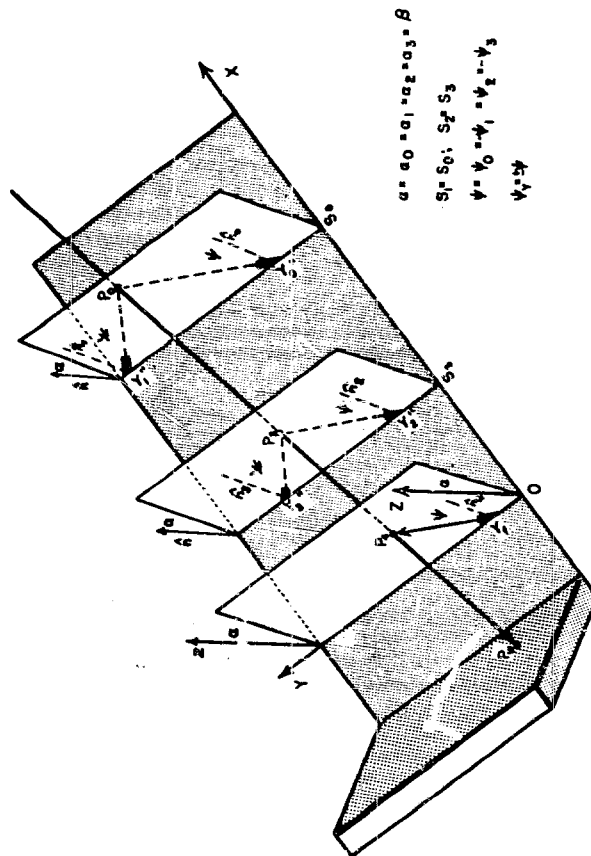
Figure 2b. Special Case of Bush-Dot Sensing System.

$$a = a_0 = a_1 = a_2 = a_3 = \beta$$

$$S_1 = S_0; \quad S_2 = S_3$$

$$\psi = \psi_0 = \psi_1 = \psi_2 = \psi_3$$

$$\psi_\gamma = \psi$$

11
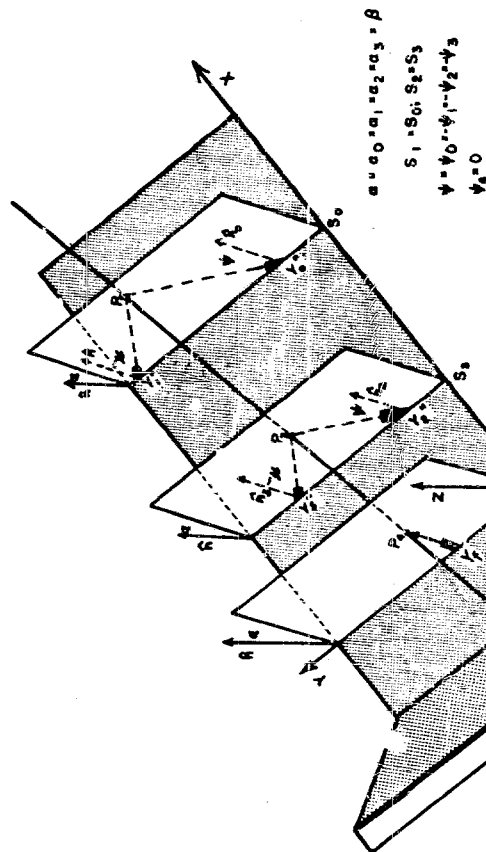
Figure 2c. Special Case of Dash-Dot Sensing System; $\psi_4 = 0$.

$\alpha = \alpha_0 = \alpha_1 = \alpha_2 = \alpha_3 = \beta$

$S_1 = S_0; \ S_2 = S_3$

$\psi = \psi_0 = \psi_1 = -\psi_2 = \psi_3$

$\psi_4 = 0$

12

3. MATHEMATICAL ANALYSIS OF A DASH-DOT SENSING SYSTEM

3.1 Problems to be Solved

In this analysis of a Dash-Dot Sensing System, there are, in general, two problems to be solved. One problem is to determine the firing-position Y_f of the appropriate shaped-charge, and the other is to determine the firing-time T_f of that charge, so that its jet may intercept the target when crossing the shaped-charge jet or β-fence. It is desired to obtain the equations or formulas to these two problems in forms suitable for rapid solving by an electronic computer.

3.2 Idealization and Coordinate System

The analysis of a Dash-Dot Sensing System made in this report is based upon the determination of two points on the target trajectory and the times of passage of those points. In analyzing the system, to a first approximation, it is helpful to idealize the detector and the armament sections. This is done by assuming that the thicknesses of the fences determined by the shaped-charge jets and by the fields of view of the detectors are infinitesimally thin and thus can be represented by geometric planes. In this connection, it is also being assumed that there is in each detector fence a detector observing the passage, and in the β-fence a properly situated shaped-charge. Actually this is not the case, the detectors and shaped-charges being fixed in position and having a finite spacing. This situation is considered in section 4. Referring to Figure 1, the plane determined by the outermost row of detectors will be designated as the α_0-fence, the next outermost row as the α_1-fence, the third row as the α_2-fence, the fourth row as the α_3-fence, and that plane determined by the shaped-charge jets as the β-fence. To further aid in the analysis, a Cartesian coordinate system is constructed in which the origin lies at one end of the row of shaped-charges. The positive y-axis lies along the row of shaped-charges and intersects their axes. The positive x-axis is perpendicular to the y-axis and extends in the direction of the detector fences. The z-axis is perpendicular to the xy-plane, and the positive direction is on that side of the xy-plane away from which the detectors and the shaped-charge jets are directed.

3.3 Basic Equations

Since the target is assumed to be traversing a rectilinear trajectory at uniform speed, then the trajectory is appropriately described by the equation of a straight line. For the equation of the

line, it will prove convenient to use the parametric form. If λ, μ, and ν are taken as the direction cosines of the straight line with respect to the x-, y- and z- axes, respectively, then the parametric form of the equation is:

$$\lambda = \frac{x - x'}{D} \ , \ \mu = \frac{y - y'}{D} \ , \ \nu = \frac{z - z'}{D} \ , \tag{1}$$

where D, the parameter, is the distance from the point $P' \equiv (x',y',z')$ to the point $P \equiv (x,y,z)$, and

$$\lambda^2 + \mu^2 + \nu^2 = 1. \tag{2}$$

The distance D may be given, for completeness, in the two forms:

$$D = + [(x - x')^2 + (y - y')^2 + (z - z')^2]^{1/2} \tag{3}$$

and

$$D = V_m (t - t'). \tag{4}$$

The second form expresses the fact that the missile is moving with uniform speed, where V_m is the speed.

In addition to the equations associated with the trajectory, there are also needed the equations of the planes formed by the idealized detector and shaped-charge jet fences. These equations are:

$$x_0 = s_0 + z_0 \tan \alpha_0 \ , \qquad \alpha_0 - \text{fence},$$

$$x_1 = s_1 + z_1 \tan \alpha_1 \ , \qquad \alpha_1 - \text{fence},$$

$$x_2 = s_2 + z_2 \tan \alpha_2 \ , \qquad \alpha_2 - \text{fence}, \tag{5}$$

$$x_3 = s_3 + z_3 \tan \alpha_3 , \qquad \alpha_3 - \text{fence},$$

$$x_4 = z_4 \tan \beta, \qquad \beta - \text{fence}.$$

The appropriate fence or plane for each equation is illustrated in Figure 1.

Should the axes of the detectors and the shaped-charges in the different fences be set at various angles ψ to the xz-plane, then the following auxiliary equations are required:

$$y_0 = y_0'' + z_0 \frac{\tan \psi_0}{\cos \alpha_0}$$

$$y_1 = y_1'' + z_1 \frac{\tan \psi_1}{\cos \alpha_1}$$

$$y_2 = y_2'' + z_2 \frac{\tan \psi_2}{\cos \alpha_2} \tag{6}$$

$$y_3 = y_3'' + z_3 \frac{\tan \psi_3}{\cos \alpha_3}$$

$$y_4 = y_4'' + z_4 \frac{\tan \psi_4}{\cos \beta} \; .$$

The general form of these equations, derived in the appendix, is given there by equation (23). In these equations, the y'''s are the y-coordinates of the detectors and the shaped-charges.

3.4 Determination of the Shaped-Charge Firing-Position

The firing-position Y_f of a shaped-charge is the y- coordinate that a shaped-charge must have if its jet is to intercept a target crossing the β-fence. This coordinate y_4'' is given by the last equation of equations (6):

$$Y_f = y_4'' = y_4 - z_4 \frac{\tan \psi_4}{\cos \beta} \; , \tag{7}$$

where y_4 and z_4 are the y- and z- coordinates of the position of passage of the β-fence by the target. To obtain y_4 and z_4, equations (1) are employed, using two known points $P_1 \equiv (x_1, y_1, z_1)$ and $P_3 \equiv (x_3, y_3, z_3)$ on the trajectory. These equations give

$$\lambda = \frac{x_3 - x_1}{D_{13}} \; , \quad \lambda = \frac{x_4 - x_1}{D_{14}} \; ,$$

$$\mu = \frac{y_3 - y_1}{D_{13}} \; , \quad \mu = \frac{y_4 - y_1}{D_{14}} \tag{8}$$

$$v = \frac{z_3 - z_1}{D_{13}} \; , \quad v = \frac{z_4 - z_1}{D_{14}}$$

where, from equations (5),

$$x_4 = z_4 \tan \beta. \tag{9}$$

From the first two equations of equation (8), there is obtained

$$\frac{x_4 - x_1}{x_3 - x_1} = \frac{D_{14}}{D_{13}} \; ; \tag{10}$$

from the second two equations,

$$\frac{y_4 - y_1}{y_3 - y_1} = \frac{D_{14}}{D_{13}}. \tag{11}$$

Upon equating the left members of equations (10) and (11) and solving for y_4, there results

$$y_4 = y_1 + \frac{x_4 - x_1}{x_3 - x_1} (y_3 - y_1). \tag{12}$$

In a similar way, making use of the first two and the last two equations of equation (8), there is obtained a relationship among the x's and z's. Then making the substitution for x_4 from equation (9) and solving for z_4, there is obtained

$$z_4 = \frac{z_1 (x_3 - x_1) - x_1(z_3 - z_1)}{(x_3 - x_1) - (z_3 - z_1) \tan \beta}. \tag{13}$$

The substitution of the values of y_4 and z_4 as given by equations (12) and (13) into equation (7) gives the firing-position Y_f of the appropriate shaped-charge. The expression for Y_f in terms of the coordinates of the two determined points on the trajectory will not be written out, since, as can be readily shown, it is quite lengthy.

3.4.1 Derivation of the Coordinates of the Trajectory Points

The coordinates of two points of the trajectory, $P_1 \equiv (x_1, y_1, z_1)$ and $P_3 \equiv (x_3, y_3, z_3)$, are derived in the appendix for three different methods for determining the target trajectory. These

methods require, in general, the use of four detector fences. These
different methods will be referred to as the First Method or Method I,
the Second Method or Method II, and the Third Method or Method III.

3.4.1.1 First Method for Determining the Trajectory

In the first method there are four detector
fences of which two are parallel to each other and the other two are
transverse. The necessary and sufficient condition, $\tan \alpha_2 -$
$\tan \alpha_0 = 0$, for parallelism is illustrated in Figure 3. The coordinates
of the first point $P_1 = (x_1, y_1, z_1)$ are

$$x_1 = s_1 + z_1 \tan \alpha_1 , \tag{14}$$

from equation (5);

$$y_1 = y_1'' + z_1 \frac{\tan \psi_1}{\cos \alpha_1} , \tag{15}$$

from equation (23) of the appendix;

$$z_1 = \frac{s_0 - s_1 (1 + k_1) + s_2 k_1}{(1 + k_1)(\tan \alpha_1 - \tan \alpha_0)} \tag{16}$$

from equation (11) of the appendix. The quantity k_1 is given by
equation (20) of the appendix, and is

$$k_1 = \frac{t_1 - t_0}{t_2 - t_1} . \tag{17}$$

For the second point $P_3 \equiv (x_3, y_3, z_3)$, there is obtained, similarly,

$$x_3 = s_3 + z_3 \tan \alpha_3, \tag{18}$$

$$y_3 = y_3'' + z_3 \frac{\tan \psi_3}{\cos \alpha_3} , \tag{19}$$

$$z_3 = \frac{s_0 - s_3(1 + k_3) + s_2 k_3}{(1 + k_3)(\tan \alpha_3 - \tan \alpha_0)} \tag{20}$$

and

$$k_3 = \frac{t_3 - t_0}{t_2 - t_3} . \tag{21}$$
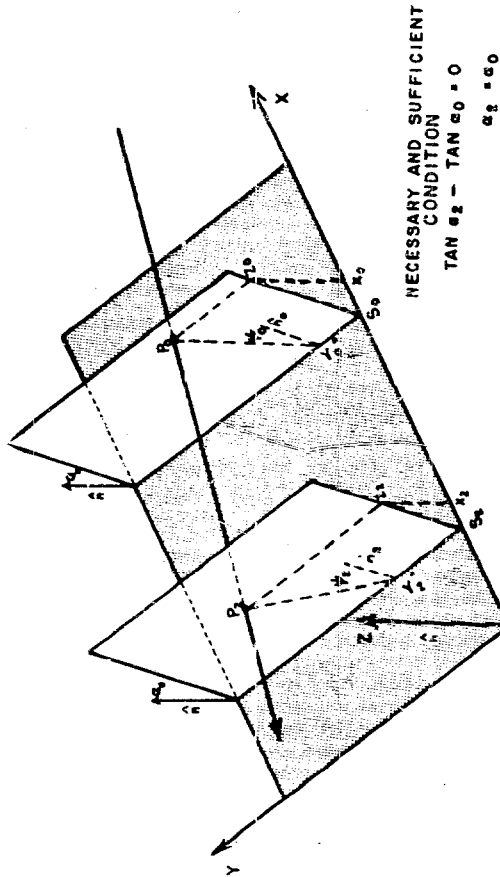
Figure 3. Illustration of the Necessary and Sufficient Condition for Theorem I and Lemma I.

18

NECESSARY AND SUFFICIENT
CONDITION

$$\frac{TAN\,\psi_2}{SIN\,\varrho_2} - \frac{TAN\,\psi_0}{SIN\,\varrho_0} = 0$$

$$\frac{TAN\,\psi_R}{SIN\,\alpha_2} = COT\,\alpha_2; \quad \frac{TAN\,\psi_0}{SIN\,\alpha_1} = COT\,\alpha_0$$

$$\therefore \gamma_2 = \gamma_0$$
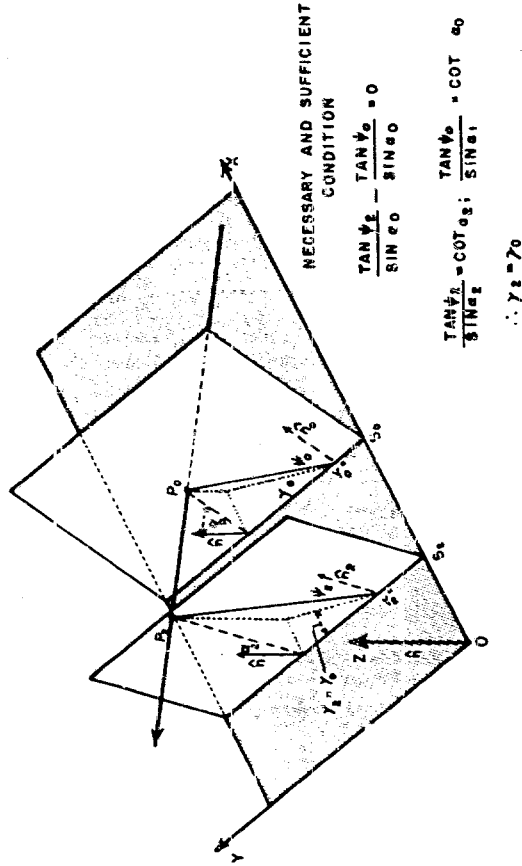
Figure 5. Illustration of the Necessary and Sufficient
Condition for Theorem II and Lemma II.

19

As shown in the appendix, there is no special case, comparable to those for the second and third methods of determining the trajectory, whereby the number of fences may be reduced in number. A special case, of a sort, does arise if it is assumed that all the trajectories are parallel to the surface S, and that all the ψ angles are equal to zero. Under these assumptions, there is needed only three planes, two parallel and one transverse, to determine the trajectory. This means that the z's are determined from equation (16), the x's from equation (5), and the y's from equation (6).

3.4.1.2 Second Method for Determining the Trajectory

For the second method, there are, in general, four fences of which two satisfy the condition:

$$\frac{\tan \psi_2}{\sin \alpha_2} - \frac{\tan \psi_0}{\sin \alpha_0} = 0. \tag{22}$$

This condition is illustrated in Figure 5 and means that the projections, of the lines of sight of the detectors in the α_0- and α_2-fences, on the xy-plane are parallel. As a result, the coordinates of the first point $P_1 \equiv (x_1, y_1, z_1)$ are

$$x_1 = \frac{y_0'' - y_1'' (1+k_1) + y_2'' k_1 - s_0 \frac{\tan \psi_0}{\sin \alpha_0} + s_1(1+k_1) \frac{\tan \psi_1}{\sin \alpha_1} - s_2 k_1 \frac{\tan \psi_2}{\sin \alpha_2}}{(1+k_1) \left(\frac{\tan \psi_1}{\sin \alpha_1} - \frac{\tan \psi_0}{\sin \alpha_0} \right)}, \tag{23}$$

for equation (23) of the appendix;

$$y_1 = y_1'' + (x_1 - s_1) \frac{\tan \psi_1}{\sin \alpha_1}, \tag{24}$$

from equation (24) of the appendix;

$$z_1 = \frac{x_1 - s_1}{\tan \alpha_1}, \tag{25}$$

from equations (5); and k_1 is given by equation (17). Similarly, there is for $P_3 \equiv (x_3, y_3, z_3)$:[1]

$$x_3 = \frac{y_0'' - y_3''(1+k_3) + y_2'' k_3 - a_0 \dfrac{\tan \psi_0}{\sin \alpha_0} + a_2(1+k_3) \dfrac{\tan \psi_3}{\sin \alpha_3} - a_2 k_3 \dfrac{\tan \psi_2}{\sin \alpha_2}}{(1+k_3)\left(\dfrac{\tan \psi_3}{\sin \alpha_3} - \dfrac{\tan \psi_0}{\sin \alpha_0}\right)} , \qquad (26)$$

$$y_3 = y_3' + (x_3 - a_3) \frac{\tan \psi_3}{\sin \alpha_3} , \qquad (27)$$

$$z_3 = \frac{x_3 - a_3}{\tan \alpha_3} \qquad (28)$$

with

$$k_3 = \frac{t_3 - t_0}{t_2 - t_3} . \qquad (29)$$

The expressions for the coordinates of the two point on the trajectory can be considerably simplified by choosing special values for the time ratio, k_1 and k_3, and the various angles involved. In particular, upon putting

$$a_3 = a_1 ,$$

$$a_2 = a_3 ,$$

$$a_0 = a_1 \qquad a_2 = a_3 \qquad (30)$$

$$\psi = \psi_0 = -\psi_1 = \psi_2 = -\psi_3 ,$$

then

$$k_1 = 0$$

$$\qquad (31)$$

$$k_3 = \infty .$$

The coordinates of P_1 become

$$x_1 = a_1 + \frac{|y_1'' - y_0''|}{2} \frac{\sin \alpha}{\tan \psi} , \qquad (32)$$

$$y_1 = \frac{y_1'' + y_0''}{2} , \qquad (33)$$

NECESSARY AND SUFFICIENT
CONDITION

$$\frac{TAN\psi_2}{COS\,a_2} - \frac{TAN\psi_0}{COS\,a_0} = 0$$
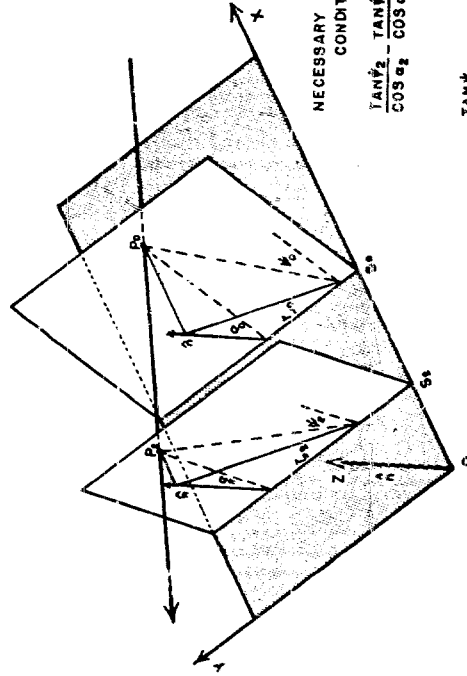
$$\frac{TAN\psi_2}{COS\,a_2} = COT\,\zeta_2 \;;\quad \frac{TAN\psi_0}{COS\,a_0} = COT\,\zeta_0$$

$$\therefore \;\; \zeta_2 = \zeta_0$$

Figure 6. Illustration of the Necessary and Sufficient
Condition for Theorem III and Lemma III.

23

$$z_1 = \frac{\left|y_1'' - y_0''\right|}{2} \ \frac{\cos \alpha}{\tan \psi} \ . \tag{34}$$

The coordinates of P_3 become

$$x_3 = s_3 + \frac{\left|y_3'' - y_2''\right|}{2} \ \frac{\sin \alpha}{\tan \psi} \ , \tag{35}$$

$$y_3 = \frac{y_3'' + y_2''}{2} \ , \tag{36}$$

$$z_3 = \frac{\left|y_3'' - y_2''\right|}{2} \ \frac{\cos \alpha}{\tan \psi} \ . \tag{37}$$

3.4.1.3 Third Method for Determining the Trajectory

For the third method, there are, in general, four fences of which two satisfy the condition:

$$\frac{\tan \psi_2}{\cos \alpha_2} - \frac{\tan \psi_0}{\cos \alpha_0} = 0. \tag{38}$$

This condition is illustrated in Figure 6 and means that the projections, of the lines of sight of the detectors in the α_0 and α_2- fences, on the yz-plane are parallel. As a result, the coordinates of the first point $P_1 \equiv (x_1, y_1, z_1)$ are

$$x_1 = s_1 + z_1 \tan \alpha_1, \tag{39}$$

from equations (5);

$$y_1 = y_1'' + z_1 \frac{\tan \psi_1}{\cos \alpha_1} \ , \tag{40}$$

from equations (6);

$$z_1 = \frac{y_0'' - y_1'' (1 + k_1) + k_1 y_2''}{(1+k_1)\left(\dfrac{\tan \psi_1}{\cos \alpha_1} - \dfrac{\tan \psi_0}{\cos \alpha_0}\right)} \ , \tag{41}$$

from equation (37) of the appendix; and k_1 is given by equation (17).
Similarly, the coordinates of the second point $P_3 = (x_3, y_3, z_3)$ are

$$x_3 = s_3 + z_3 \tan \alpha_3, \tag{42}$$

$$y_3 = y_3'' + z_3 \frac{\tan \psi_3}{\cos \alpha_3}, \tag{43}$$

$$z_3 = \frac{y_0'' - y_3'' (1 + k_3) + k_3 y_2''}{(1 + k_3)\left(\dfrac{\tan \psi_3}{\cos \alpha_3} - \dfrac{\tan \psi_0}{\cos \alpha_0}\right)}, \tag{44}$$

with

$$k_3 = \frac{t_3 - t_0}{t_2 - t_3}. \tag{45}$$

As with the second method, the expressions
for the coordinates of the two points on the trajectory can be considerably
simplified by choosing special values for the time ratios, k_1 and k_3, and
the various angles involved. In particular, if the values given by
equations (30) are used, the coordinates of P_1 become

$$x_1 = s_1 + \frac{\left| y_1'' - y_0'' \right|}{2} \frac{\sin \alpha}{\tan \psi}, \tag{46}$$

$$y_1 = \frac{y_1'' + y_0''}{2}, \tag{47}$$

$$z_1 = \frac{\left| y_1'' - y_0'' \right|}{2} \frac{\cos \alpha}{\tan \psi}; \tag{48}$$

and the coordinates of P_3 become

$$x_3 = s_3 + \frac{\left| y_3'' - y_2'' \right|}{2} \frac{\sin \alpha}{\tan \psi}, \tag{49}$$

$$y_3 = \frac{y_3'' + y_2''}{2}, \tag{50}$$

$$z_3 = \frac{|y_3'' - y_2''|}{2} \quad \frac{\cos \alpha}{\tan \psi} . \tag{51}$$

3.4.2 Determination of the Coordinates of the Point of Passage of the Shaped-Charge Fence

To obtain the coordinates, in the general case, of the point of passage of the shaped-charge fence by the target, the general expressions for the coordinates of the two points, P_1 and P_3, are used. The values are used with equation (13) to give z_4; this value of z_4 is used in equation (9) to give x_4 in terms of the general coordinates. Upon substituting this value of x_4 and the values of the x- and y-coordinates of the two points into equation (12), the value of y_4 is obtained.

3.4.2.1 Point of Passage of Shaped-Charge Fence, Using Special Case of Method I.

The expressions for the coordinates of the point of passage of the shaped-charge fence can be simplified considerably by assuming special target trajectories or using special methods for determining the trajectory. The first method for determining the trajectory yields simple formulas for the coordinates of the point of passage of the β- or shaped-charge fence, if the trajectories are assumed to be parallel to the surface S, that is parallel to the yz- plane, if $\psi_4 = \psi_2 = \psi_1 = \psi_0 = 0$, and if $\beta = \alpha_2 = \alpha_0$. The condition that the trajectories be parallel to the xy- plane means that $z_4 = z_2 = z_1 = z_0$. Under these conditions, it is not necessary to use the α_3- or fourth detector fence, for the first three fences give sufficient information. From equations (13), (16) and (17) there is obtained

$$z_4 = \frac{s_0 - s_1}{\tan \alpha_1 - \tan \alpha_0} \quad \frac{t_2 - t_1}{t_2 + t_1} - \frac{s_1 - s_2}{\tan \alpha_1 - \tan \alpha_0} \quad \frac{t_1 - t_0}{t_2 + t_1} ; \tag{52}$$

and from equation (9) and equation (52),

$$x_4 = \frac{(s_0 - s_1) \tan \alpha_0}{\tan \alpha_1 - \tan \alpha_0} \quad \frac{t_2 - t_1}{t_2 + t_1} - \frac{(s_1 - s_2) \tan \alpha_0}{\tan \alpha_1 - \tan \alpha_0} \quad \frac{t_1 - t_0}{t_2 + t_1} . \tag{53}$$

As the fourth detector fence is now omitted, equation (12) can no longer be used since x_3 and y_3 are unknown. By

following the same procedure as was used to derive equation (12), but using the points P_0 and P_2, there is obtained

$$y_4 = y_0 + \frac{x_4 - x_0}{x_2 - x_0} (y_2 - y_0) \ . \tag{54}$$

Upon making the proper substitution from equations (5) and (53),

$$y_4 = \frac{s_0}{s_0 - s_2} y_2 - \frac{s_2}{s_0 - s_2} y_0 \ . \tag{55}$$

3.4.2.2 Point of Passage of Shaped-Charge Fence, Using Special Cases of Methods II and III.

If

$$\beta = \alpha , \tag{56}$$

and since the special cases of the second and third methods for determining the trajectory are identical, then for these two methods the coordinates of P_4 become

$$x_4 = \frac{s_1 \sin \alpha}{(s_1 - s_3) \tan \psi} \frac{|y_3'' - y_2''|}{2} - \frac{s_3 \sin \alpha}{(s_1 - s_3) \tan \psi} \frac{|y_1'' - y_0''|}{2} \tag{57}$$

$$y_4 = \frac{s_1}{s_1 - s_3} \frac{y_3'' + y_2''}{2} - \frac{s_3}{s_1 - s_3} \frac{y_1'' + y_0''}{2} , \tag{58}$$

$$z_4 = \frac{s_1 \cos \alpha}{(s_1 - s_3) \tan \psi} \frac{|y_3'' - y_2''|}{2} - \frac{s_3 \cos \alpha}{(s_1 - s_3) \tan \psi} \frac{|y_1'' - y_0''|}{2} \ . \tag{59}$$

3.4.3 Determination of Shaped-Charge Firing-Position For Special Cases

The shaped-charge firing-position Y_f, in the general case, is obtained by substituting the general values of y_4 and z_4 into equation (7). To obtain the firing-position, when the trajectories are parallel to the xy-plane and are determined by the first method, it is to be noted that in equation (7) $\psi_4 = 0$ and thus from equation (54)

$$Y_f = y_4 = \frac{s_o}{s_o - s_2} \, y_2 - \frac{s_2}{s_o - s_2} \, y_o \, . \tag{60}$$

If the special cases of the second and third methods are used, then substituting the values of y_4 and z_4 from equations (58) and (59) into equation (7),

$$Y_f = \frac{s_1}{s_1 - s_3} \left[\frac{y_3'' + y_2''}{2} - \frac{|y_3'' - y_2''|}{2} \frac{\tan \psi_4}{\tan \psi} \right]$$

$$- \frac{s_3}{s_1 - s_3} \left[\frac{y_1'' + y_o''}{2} - \frac{|y_1'' - y_o''|}{2} \frac{\tan \psi_4}{\tan \psi} \right] \, . \tag{61}$$

For equation (61) there are the two special conditions:

$$\psi_4 = \pm \psi \tag{62}$$

and

$$\psi_4 = 0 \, . \tag{63}$$

If condition (62) is used, equation (61) becomes

$$Y_f = \frac{s_1}{s_1 - s_3} \left[\frac{y_3'' - y_2''}{2} \mp \frac{|y_3'' - y_2''|}{2} \right]$$

$$- \frac{s_3}{s_1 - s_3} \left[\frac{y_1'' + y_o''}{2} \mp \frac{|y_1'' - y_o''|}{2} \right] \, , \quad \psi_4 = \pm \psi. \tag{64}$$

If condition (63) is used, equation (61) becomes

$$Y_f = \frac{s_1}{s_1 - s_3} \frac{y_3'' + y_2''}{2} - \frac{s_3}{s_1 - s_3} \frac{y_1'' + y_o''}{2}, \quad \psi_4 = 0. \tag{65}$$

3.5 Determination of Shaped-Charge Firing-Time

The second problem to solve is the determination of the firing-time T_f of the appropriate shaped-charge, so that its jet will intercept the target when crossing the β-fence. For the firing-time T_f, the general formula is

$$T_f = t_4 - \tau - \delta; \tag{66}$$

SECRET

where t_4 is the time of passage of the β- fence by the target; τ is the interval of time required by the jet to traverse the distance from the shaped-charge to the target in the β- fence; and δ is a time interval representing, collectively, all other time delays inherent in the system.

From equations (1) and (4), there are readily obtained the formulas:

$$t_4 = t_1 + \frac{x_4 - x_1}{x_3 - x_1} (t_3 - t_1) \tag{67a}$$

for the general case, and

$$t_4 = t_0 + \frac{x_4 - x_0}{v_2 - v_0} (t_2 - t_0) \tag{67b}$$

for a special case. The simple geometrical relationships existing between z_4, the z- coordinate of the point of passage of the β- fence, and q_4, the distance between the appropriate shaped-charge and the point of missile passage in the β- fence, permits the transit-time τ to be easily obtained. For example, considering Figure 4, β now taking the place of the angle α,

$$z_4 = p_4 \cos \beta \tag{68}$$

and

$$p_4 = q_4 \cos \psi_4 \tag{69}$$

where p_4 is the distance from the xy-plane to the point of passage. By eliminating p_4 from these two equations, there is obtained

$$q_4 = \frac{z_4}{\cos \beta \cos \psi_4} \tag{70}$$

Since the transit-time τ, by definition, is

$$\tau = \frac{q_4}{V_c} , \tag{71}$$

where V_c is the velocity of the shaped-charge jet, then using the value of q_4 from equation (70) in equation (71),

$$\tau = \frac{z_4}{V_c \cos \beta \cos \psi_4} . \tag{72}$$

* See Appendix for Figure 4.

28 SECRET

Thus the firing-time T_f as given by equation (66), using equations (67) and (72) can be determined in terms of the positions and the times of passage of the detector fences.

3.5.1 Determination of Transit Time for Special Cases

For the special case using Method I, $\beta = \alpha_o$ and $\psi_4 = 0$. This gives, together with the value of z_4 from equation (52), for the transit time,

$$\tau = \frac{s_o - s_1}{V_c \cos \alpha_o (\tan \alpha_1 - \tan \alpha_o)} \frac{t_2 - t_1}{t_2 + t_1}$$
$$- \frac{s_1 - s_2}{V_c \cos \alpha_o (\tan \alpha_1 - \tan \alpha_o)} \frac{t_1 - t_o}{t_2 + t_1} .$$
(73)

For the special cases, using Methods II and III, $\beta = \alpha_3 = \alpha_o = \alpha$. With $\psi_4 = \pm \psi$ and using the value of z_4 from equation (56), equation (72) gives

$$\tau = \frac{s_1}{V_c (s_1 - s_3) \sin \psi} \frac{|y_3'' - y_2''|}{2} - \frac{s_3}{V_c (s_1 - s_3) \sin \psi} \frac{|y_1'' - y_o''|}{2} .$$
(74a)

If $\psi_4 = 0$,

$$\tau = \frac{s_1}{(s_1 - s_3) V_c \tan \psi} \frac{|y_3'' - y_2''|}{2} - \frac{s_3}{(s_1 - s_3) V_c \tan \psi} \frac{|y_1'' - y_o''|}{2} .$$
(74b)

3.5.2 Determination of Time of Passage of Shaped-Charge Fence for Special Cases

To determine the time of passage of the shaped-charge fence for the special case of Method I, the conditions are $\beta = \alpha_2 = \alpha_o$ and $\psi_4 = \psi_2 = \psi_1 = \psi_c = 0$. Under these conditions equations (67b) and (5) give

$$t_4 = \frac{s_o}{s_o - s_2} t_2 - \frac{s_2}{s_o - s_2} t_o$$
(75a)

or

$$t_4 = t_o + \frac{s_o}{s_o - s_2} (t_2 - t_o) .$$
(75b)

To obtain t_4 for the special cases of Method II and III, equations (57), (49), and (46) are used. These give from equations (57) and (46),

$$x_4 - x_1 = \frac{s_1}{s_1 - s_3} \left\{ -(s_1 - s_3) + \left[\frac{\left| y_3'' - y_2'' \right|}{2} - \frac{\left| y_1'' - y_0'' \right|}{2} \right] \frac{\sin \alpha_o}{\tan \psi} \right\}, \qquad (76)$$

and from equations (49) and (46),

$$x_3 - x_1 = -(s_1 - s_3) + \left[\frac{\left| y_3'' - y_2'' \right|}{2} - \frac{\left| y_1'' - y_0'' \right|}{2} \right] \frac{\sin \alpha_o}{\tan \psi} . \qquad (77)$$

Upon substituting the values of these differences into equations (67a),

$$t_4 = t_1 + \frac{s_1}{s_1 - s_3} (t_3 - t_1). \qquad (78)$$

3.5.3 Determination of Shaped-Charge Firing-Time for Special Cases

Upon substituting the value of τ from equation (73) and the value of t_4 from equation (75) into equation (66), there is obtained, for the special case of Method I, for the firing-time,

$$T_f = t_0 + \frac{s_o}{s_o - s_2} (t_2 - t_0)$$

$$- \frac{s_o - s_1}{V_c(\tan \alpha_1 - \tan \alpha_o)\cos \alpha_o} \frac{t_2 - t_1}{t_2 + t_1} \qquad (79)$$

$$+ \frac{s_1 - s_2}{V_c(\tan \alpha_1 - \tan \alpha_o)\cos \alpha_o} \frac{t_1 - t_0}{t_2 + t_1} - \delta .$$

For the special cases of Methods II and III there is obtained, upon substituting the value of τ from equation (74a) and the value of t_4 from equation (78) into equation (66), for the firing-time

$$T_f = t_1 + \frac{s_1}{s_1 - s_3} (t_3 - t_1) - \frac{s_1}{(s_1 - s_3)V_c \sin \psi} \frac{\left| y_3'' - y_2'' \right|}{2} \qquad (80a)$$

$$+ \frac{s_3}{(s_1 - s_3) V_c \sin \psi} \frac{\left| y_1'' - y_0'' \right|}{2} - \delta . \qquad \psi_4 = \pm \psi .$$

With the value of τ from equation (74b),

$$T_f = t_1 + \frac{s_1}{s_1 - s_3}(t_3 - t_1) - \frac{s_1}{(s_1 - s_3)V_c \tan\psi} \frac{|y_3'' - y_2''|}{2}$$
$$+ \frac{s_3}{(s_1 - s_3)V_c \tan\psi} \frac{|y_1'' - y_0''|}{2} - \delta. \quad \psi_4 = 0. \tag{80b}$$

3.6 Summary of Special Cases

In summary, the special cases considered are trajectories parallel to the xy-plane when using Method I, and a system consisting of two detector fences and one shaped-charge jet fence when using Methods II and III.

Special Case I: In this case there are three detector fences of which two are parallel to each other and the third is transversely placed with respect to the two. All the ψ angles of the detectors are zero, that is lines of sight of the detectors in each row are perpendicular to that row. Also the ψ angles of the shaped-charge jet axes are zero, and $\beta = \alpha_2 = \alpha_0$. The missile trajectories are assumed to be parallel to the surface S or the xy-plane. Under these conditions, the firing-position is

$$Y_f = \frac{s_0}{s_0 - s_2} Y_2 - \frac{s_2}{s_0 - s_2} y_0, \tag{81-60}$$

and the firing-time is

$$T_f = t_0 + t \frac{s_0}{s_0 - s_2}(t_2 - t_0) - \frac{s_0 - s_1}{V_c(\tan \alpha_1 - \tan \alpha_0)\cos \alpha_0} \frac{t_2 - t_1}{t_2 + t_1}$$
$$+ \frac{s_1 - s_2}{V_c(\tan \alpha_1 - \tan \alpha_0)\cos \alpha_0} \frac{t_1 - t_0}{t_2 + t_1} - \delta. \tag{82-79}$$

Special Case I is illustrated in Figure 2a.

Special Case II: In this case, which is derived from Methods II and III, there are two detector fences and one shaped-charge jet fence, all the fences being set at the same angle α with respect to the normal to the xy-plane. In each detector fence each detector observes in two directions — the angle of one direction is ψ and that of the other is $-\psi$. There are two arrangements of the shaped-charge jets. In one the axes of the shaped-charges make an angle $\pm\psi$ with the normal to the shaped-charge row. In the other the angle ψ is equal to zero. For $\psi = \psi_0 = -\psi_1 = \psi_2 = -\psi_3$ and $\psi_4 = \pm\psi$, the firing-position, from equation (64), is

$$Y_f = \frac{s_1}{s_1 - s_3} \left[\frac{y_3'' + y_2''}{2} \mp \frac{|y_3'' - y_2''|}{2} \right] \tag{83-64}$$

$$- \frac{s_3}{s_1 - s_3} \left[\frac{y_1'' + y_0''}{2} \mp \frac{|y_1'' - y_0''|}{2} \right] \; , \; \psi_4 = \pm\psi.$$

For the firing-time, from equation (80a),

$$T_f = t_1 + \frac{s_1}{s_1 - s_3}(t_3 - t_1) - \frac{s_1}{(s_1 - s_3)V_c \sin\psi} \; \frac{y_3'' - y_2''}{2}$$

$$+ \frac{s_3}{(s_1 - s_3)V_c \sin\psi} \; \frac{|y_1'' - y_0''|}{2} - \delta, \; \psi_4 = \pm\psi. \tag{84-80a}$$

This special case of Methods II and III is illustrated in Figure 2b. If $\psi_4 = 0$, then, from equation (65),

$$Y_f = \frac{s_1}{s_1 - s_3} \; \frac{y_3'' + y_2''}{2} - \frac{s_3}{s_1 - s_3} \; \frac{y_1'' + y_0''}{2}, \; \psi_4 = 0; \tag{85-65}$$

and from equation (80b),

$$T_f = t_1 + \frac{s_1}{s_1 - s_3}(t_3 - t_1) - \frac{s_1}{(s_1 - s_3)V_c \tan\psi} \; \frac{y_3'' - y_2''}{2}$$

$$+ \frac{s_3}{(s_1 - s_3)V_c \tan\psi} \; \frac{|y_1'' - y_0''|}{2} - \delta, \; \psi_4 = 0. \tag{86-80b}$$

This special case of Methods II and III is illustrated in Figure 2b.

4. ERROR ANALYSIS

4.1 Approximating the Operation of an Actual System.

The operation of an actual system may be approximated by analyzing an ideal system incorporating errors. These errors arise from those inherent in the computer and in variations in the data fed to the computer. Regarding these errors, it will be assumed that those inherent in the computer have the same weight as those due to variations of the coordinates of the points of passage of the fences by the target. Thus variations in all terms containing the factor $1/V_c$ will be considered as being negligible; also it will be assumed that all determinations of times of passage are very precise and any variations in time are due to variations of the coordinates of the points of passage of the fences.

Under these assumptions and if in case II, t_1 and t_3 are changed to t_0 and t_2 respectively, and if s_1 and s_3 are changed to s_0 and s_4 respectively, then case I and case II become, from an error viewpoint, identical. Consequently only case I will be analyzed in detail. The error in firing-position Y_f, due to small variations of the various parameters, is given by the total differential of Y_f (equation (81)). As can be shown

$$\left|dY_f\right|_{max} = \left|y_2 - y_0\right| \frac{1+a}{1-a^2} \left|\frac{ds}{s_0}\right| + \frac{1+a}{1-a} \left|dy\right|, \tag{87}$$

where $\left|dY_f\right|_{max}$ is the maximum absolute error in the firing-position Y_f; $\left|y_2 - y_0\right|$ is the absolute value of the difference of the ideal coordinates of the positions of passage in the two fences; a is the ratio of the distance s_2 of the second fence and the distance s_0 of the first fence from the shaped-charges; and $\left|dy\right|$ is the absolute value of the variations of the ideal coordinates of the points of passage. The maximum absolute values of ds_0 and ds_2 are assumed equal to each other; the same assumption is made also with respect to dy_0 and dy_2.

Instead of determining errors in the firing-time T_f, it is preferable to determine those in t_4, the time of passage of the shaped-charge fence, since variations in those terms containing the factor $1/V_c$ are assumed to be negligible. Thus there is obtained for the error in the time of passage of the shaped-charge jet fence,

$$\left|dt_4\right|_{max} = 2\, t_4 \frac{1+a}{1-a} \left|\frac{ds}{s_0}\right|. \tag{88}$$

In this formula, a and $\left|ds/s_0\right|$ have the same meanings as in equation (87). If the errors in the computer can be neglected, then the value of $\left|dt_4\right|_{max}$ as given by equation (88) will be reduced one-half.
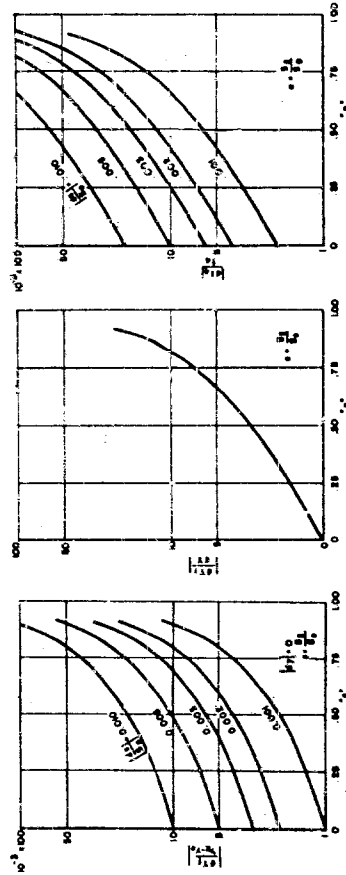
Figure 9. $\dfrac{dt_4}{t_4}$ vs. a.

Figure 8. $\left|\dfrac{dY_f}{dY}\right|$ vs. a.

Figure 7. $\left|\dfrac{dY_f}{V_2 - Y_0}\right|$ vs. a.

34

Figures 7 and 8 are graphs which may be used to readily evaluate equation (87). These graphs were constructed by separating equation (87) into two parts. Figure 7 gives $|dY_f/y_2-y_0|$ as a function of a with $|ds/s_0|$ considered as a parameter and $|dy| = 0$. Figure 8 gives $|dY_f/dy|$ as a function of a with $|ds/s_0| = 0$. Figure 9 illustrates equation (88), where $|dt_4/t_4|$ is plotted against a.

It is to be noted that equations (87) and (88) take into consideration errors arising due to the target being detected before and after the ideal fence, and to either side of a detector. If, as probably is the actual case, the errors in passage can be biased to the entering side of the fences and if an averaging circuit is used to determine the lateral points of passage, then errors in t_4 and in Y_f can be reduced considerably.

4.2 Example of Errors

As an example in the use of these graphs, consider a target having a velocity of 6×10^4 cm/sec; take a $= s_2/s_0 = 0.30$; take $|ds/s_0| = 0.010$, $|dy| = 5cm$, $|y_3 - y_1| = 300$ cm; and $t_4 = 8.5 \times 10^{-3}$ sec. From Figure 7, there is obtained

$$\left|\frac{dY_f}{y_3-y_1}\right|_1 = 14 \times 10^{-3} \tag{89}$$

the subscript 1 referring to the first part of the error in dY_f and 2 referring to the second part.

Since $|y_3 - y_1| = 300$ cm, then $|dY_f|_1 = 4.2$ cm. From Figure 8, for a $= 0.30$, $|dY_f/dy|_2 = 1.84$. Since $|dy| = 5$ cm, then $|dY_f|_2 = 9.2$ cm. Upon combining the two parts, there is obtained

$$|dY_f|_{max} = |dY_f|_1 + |dY_f|_2 , \tag{90}$$

giving $|dY_f|_{max} = 13.4$ cm or $dY_{f\ max} = \pm 13.4$ cm.

With respect to the time of passage t_4, Figure 9 is used. For a $= 0.30$ and $|ds/s_0| = 0.010$, $|dt_4/t_4|_{max} = 37 \times 10^{-3}$. Since $t_4 = 8.5 \times 10^{-3}$ sec, then $|dt_4|_{max} = 3.145 \times 10^{-4}$ sec.

Let D be the distance along the target trajectory; then since

$$dD = V_m\ dt_4 \tag{91}$$
$$= (6 \times 10^4) \times (3.145 \times 10^{-4}),$$

35

$$|dD|_{max} = 18.87 \text{ cm} \tag{92}$$

or

$$dD_{max} = \pm 18.87 \text{ cm} \tag{93}$$

If the errors inherent in the computer can be neglected, then

$$dD_{max} = \pm 9.43 \text{ cm}. \tag{94}$$

If, as has been noted, the errors in points of passage can be biased and averaged, then the errors in Y_r, t_4 and D can be reduced considerably.

V. RESOLVING ABILITY OF A DASH-DOT SENSING SYSTEM

To make a Dash-Dot Sensing System highly effective, it must have the ability to distinguish several targets passing, at most, the fences simultaneously but having different positions of passage. This ability is defined as the resolving ability of the system. The system analyzed in this report does not have this ability. A system having at least a simple resolving ability, i.e., distinguishing two targets, would, no doubt, require more fences and a complicated computer.

Although the present system does not have lateral resolving ability, it has a certain amount of time resolving ability. Thus if the maximum time of transit from the first detector to the shaped-charge jet fence is T_4 and the reset time of the computer is T_r, then the resolving time T_R is

$$T_R = T_4 + T_r .\tag{95}$$

Equation (95) means that if two targets are separated in time, that is one following the other by the interval T_R then the Dash-Dot Sensing System can discern them as separate targets, with the computer effectively performing the necessary computations.

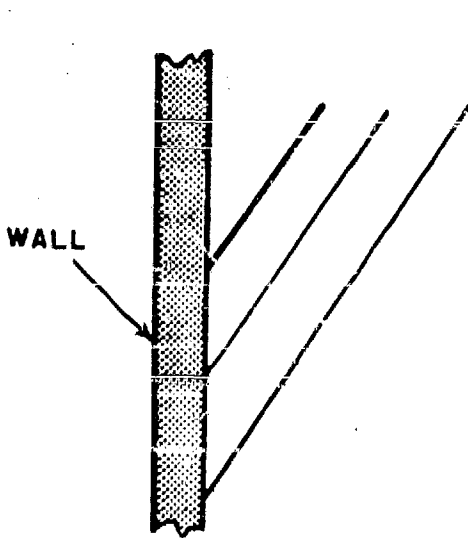Figure 11. Flush Mounting of System.

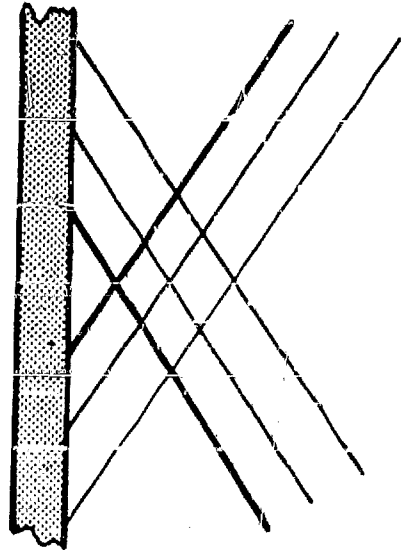Figure 12. Arrangement to Provide Mutual Protection

OUTRIGGER (TYP)
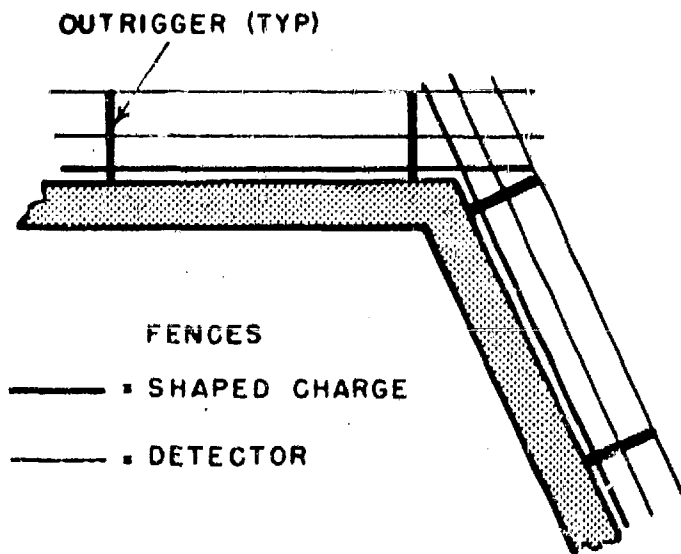
FENCES

——— ▪ SHAPED CHARGE

——— ▪ DETECTOR

Figure 10. Overlapping of Systems to Protect Corners.

6. SPECIAL ARRANGEMENTS OF DASH-DOT SENSING SYSTEM

Besides serving as a means to protect a wall from damage, various arrangements of one or more Dash-Dot Sensing Systems can be used to minimize or eliminate damage to the systems themselves and to corners of fortifications, vehicles and vessels. Figure 10 illustrates an arrangement of Dash-Dot Sensing Systems to provide protection to the corner of a structure. In this arrangement, the two systems overlap each other at the corner. Thus a target approaching the corner will be intercepted by at least one of the systems.

A Dash-Dot Sensing System using out-riggers to support the fences is vulnerable to possible direct hits and also, if used on vehicles, to collisions with protruding objects such as trees, tree stumps, boulders, barriers, etc. To eliminate these possibilities and render at least only part of the system vulnerable, an arrangement with respect to a wall is shown in Figure 11. Here the system is flush mounted on the wall or embedded in the wall. This arrangement still leaves the various parts of the system separately vulnerable, To provide, more or less, complete protection for such a system, two such systems could be arranged as shown in Figure 12. Here the two systems not only protect the wall, but also provide protection to each other from a directly approaching target.

It is to be observed that of the various armament and detector arrangements of a Dash-Dot Sensing System, an arrangement as illustrated in Figure 2a is more effective in protecting a wall than such arrangements as illustrated in Figures 2b and 2c. This is so since the system of Figure 2a can determine the positions of a target up to the ends of the fences, whereas the systems in Figures 2b and 2c can not do so. In Figures 2b and 2c, if a target passes near the end of a fence it is seen that only part of the detectors observe the passage. To determine the point of passage, the equations for the point require the observation from two directions.

7. ACKNOWLEDGMENT

The writer appreciates the helpful discussions with Dr. H. W. Kohler concerning various aspects of the Dash-Dot Sensing System. Before the general analysis was made, he pointed out the simplicity of the formulas for the special cases. It was at his suggestion that the general analysis was undertaken. A number of helpful suggestions were made by Dr. H. W. Straub and Mr. B. Zendle.

8. APPENDIX

8.1 Determination of the Target Trajectory

The determination of a target trajectory by a Dash-Dot Sensing System is based upon using, at most, four fences formed by the spaces observed by four rows of photosensitive detectors. In this appendix, the fences will be idealized, that is assumed to have infinitesimal thicknesses, and referred to as planes. If there exist relationships among the coordinates of each position of passage of the planes, then in general, there are three methods by which the trajectory may be determined. The three methods resolve themselves upon the fact that in each method the projections on a given coordinate plane of the directions of observation of the detectors in two of the planes are parallel.

8.2 First Method for Determining the Trajectory

The basis of the first method for determining the target trajectory is the relationship existing between the x- and z-coordinates of each position of passage of the planes. The first method may be summarized in the following theorem:

Theorem I: A target is traversing a rectilinear trajectory with uniform speed. The y-coordinates of the positions of the activated detectors in the planes and the times of passage of the planes of a set of planes are observed. All the planes of the set are parallel to the y-axis. To determine the trajectory of the target, it is in general necessary and sufficient to have the set of planes composed of, at most, four, noncoincident planes of which two are parallel to each other and the remaining two are transverse.

This theorem is a special case of the system as illustrated in Figure 1, in which any two of the detector fences or planes are made parallel to each other, e.g., $\alpha_2 = \alpha_0$. The necessary and sufficient condition is illustrated in Figure 3. Since the trajectory is by assumption a straight line along which the missile is moving at uniform speed, then the theorem is thus equivalent to the determination of a straight line along which distances are proportional to the time required by the target (point target) to traverse those distances. Before proving the theorem, the following lemma will be proved:

Lemma I: Three, noncoincident planes, parallel to the y-axis with one of the planes being transverse to the other two, divide a transverse line into a given ratio. For the x- and z-coordinates of the point of intersection of the line and the transverse plane to be independent of the points of intersection of the line and the other two planes, it is necessary and sufficient for the two planes to be parallel to each other.
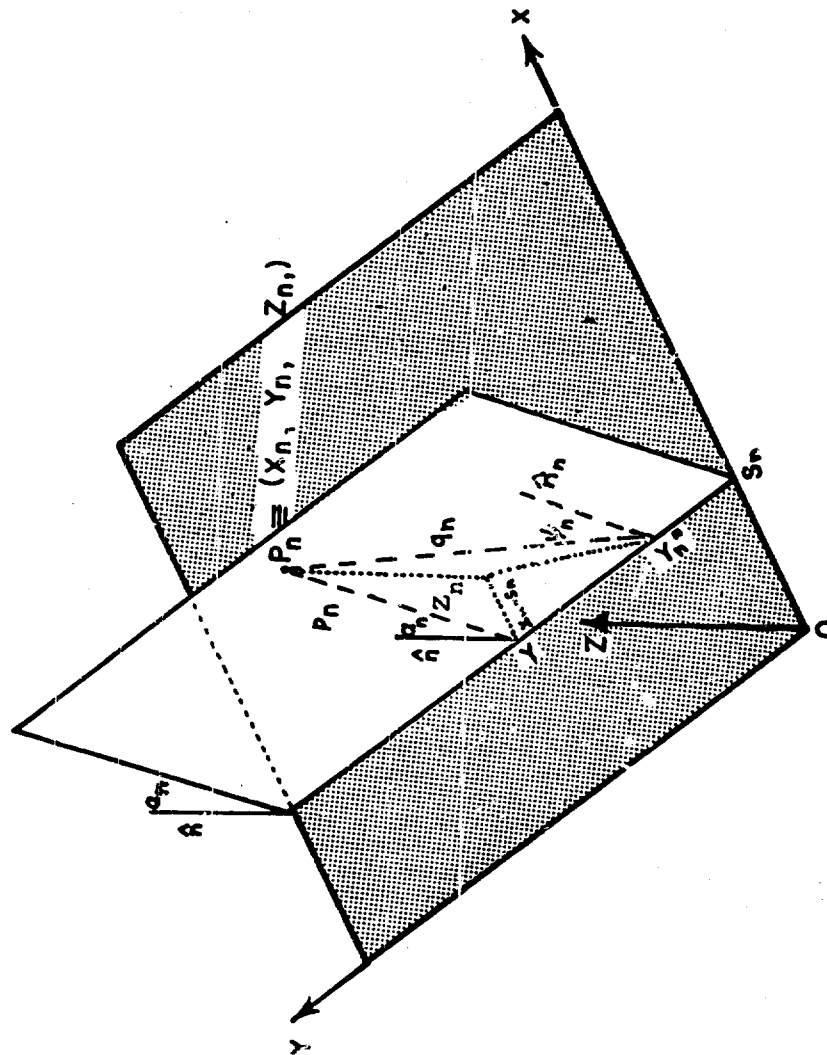
Figure 4. Illustration of the Angles ψ_n and α_n and the Distances p_n and q_n in the Different Planes.

42

Proof of Lemma I: (Refer to Figure 13). Let the parametric equations of the straight line be

$$\lambda = \frac{x - x'}{D}, \quad \mu = \frac{y - y'}{D}, \quad \nu = \frac{z - z'}{D}, \tag{1}$$

where λ, μ, and ν are the direction cosines of the line with reference to the x, y, and z axes, respectively. Without loss of generality, the equations of the three planes may be taken as

$$x_0 = s_0 + z_0 \tan \alpha_0 \qquad\qquad \alpha_0\text{-plane}$$

$$x_1 = s_1 + z_1 \tan \alpha_1 \qquad\qquad \alpha_1\text{-plane} \tag{2}$$

$$x_2 = s_2 + z_2 \tan \alpha_2 \qquad\qquad \alpha_2\text{-plane},$$

where $\alpha_1 \neq \alpha_0$, $\alpha_1 \neq \alpha_2$ and $s_0 \neq s_2$, but s_1 is unrestricted. Let the distance along the line from the point $P_0 = (x_0, y_0, z_0)$, the point of intersection of the line and the first plane, to the point $P_1 = (x_1, y_1, z_1)$, the point of intersection of the line and the second plane, be D_{01}; similarly, let the distance from P_1 to $P_2 = (x_2, y_2, z_2)$, the point of intersection of the line and the third plane, be D_{12}. Then

$$k = \frac{D_{01}}{D_{12}}, \tag{3}$$

where k is the given ratio.

Using the first two points on the line, given by the first two equations of equations (2), the first of equations (1) may be written

$$\lambda = \frac{s_1 + z_1 \tan \alpha_1 - (s_0 + z_0 \tan \alpha_0)}{D_{01}}, \tag{4}$$

and with the second and third points, given by the second and third equations of equations (2),

$$\lambda = \frac{s_2 + z_2 \tan \alpha_2 - (s_1 + z_1 \tan \alpha_1)}{D_{12}}. \tag{5}$$

With the third of equations (1), there is obtained

$$\nu = \frac{z_1 - z_0}{D_{01}} \tag{6}$$

and

$$\nu = \frac{z_2 - z_1}{D_{12}}. \tag{7}$$

Equating the right members of equations (4) and (5) and using the relationship expressed in equation (3), then

$$\frac{s_1 + z_1 \tan \alpha_1 - (s_0 + z_0 \tan \alpha_0)}{s_2 + z_2 \tan \alpha_2 - (s_1 + z_1 \tan \alpha_1)} = k. \tag{8}$$

Equating the right members of equations (6) and (7), using equations (3), and solving for z_0,

$$z_0 = z_1 (1 + k) - z_2 k. \tag{9}$$

Equations (8) and (9) are two independent relationships involving the four variables z_0, z_1, z_2 and k. In each equation, if any three of the variables have given values, then the fourth is determined. Considering the two equations simultaneously, then upon eliminating one of the variables, the resulting equation involves only the remaining three variables. Any two of these variables may be taken as the independent ones with the third being the dependent variable. In what follows, z_1 is taken as the dependent variable, and z_2 and k as the independent ones. Upon substituting the value of z_0 from equation (9) into equation (8), and solving for z_1,

$$z_1 = \frac{s_0 - s_1 (1 + k) + s_2 k}{(1 + k)(\tan \alpha_1 - \tan \alpha_0)} + z_2 k \frac{\tan \alpha_2 - \tan \alpha_0}{(1 + k)(\tan \alpha_1 - \tan \alpha_0)}. \tag{10}$$

To show, that it is sufficient to have the two planes parallel for z_1 to be independent of z_2 and consequently independent of x_2, let $\alpha_2 = \alpha_0$. Then from equation (10), it is seen that

$$z_1 = \frac{s_0 - s_1 (1 + k) + s_2 k}{(1 + k)(\tan \alpha_1 - \tan \alpha_0)} , \qquad (11)$$

which does not depend upon z_2 or x_2. Since x_1 is related to z_1, as shown by the second of equations (2), then x_1 is likewise independent of x_2 and z_2. Also, x_1 and z_1 are independent of x_0 and z_0, since they do not appear in equation (11).

To show that it is necessary to have the two planes parallel if x_1 and z_1 are independent of x_2 and z_2, write equation (10) for two values of z_2:

$$z_1 = A + B (\tan \alpha_2 - \tan \alpha_0) z_2' \qquad (12)$$

$$z_1 = \bar{A} + \bar{B} (\tan \alpha_2 - \tan \alpha_0) z_2'', \qquad (13)$$

where

$$A = \frac{s_0 - s_1 (1 + k) + s_2 k}{(1 + k)(\tan \alpha_1 - \tan \alpha_0)} \qquad (14)$$

and

$$B = \frac{k}{(1 + k)(\tan \alpha_1 - \tan \alpha_0)} \qquad (15)$$

Upon subtracting equation (13) from equation (12),

$$0 = B (\tan \alpha_2 - \tan \alpha_0)(z_2' - z_2''). \qquad (16)$$

Since B is not equal to zero, and z_2' is not equal to z_2'', then for the right member of equation (16) to be equal to zero, α_2 must equal α_0 or differ from it by $n\pi$ radians, where n is an integer. Either condition means that the two planes are parallel.

Proof of Theorem I: To prove the theorem, take three of the planes of which two are parallel to each other and the third transverse. Since distances along the straight line trajectory are proportional to the times required by the missile (point missile) to traverse those distances, that is

$$D = V_m (t - t'),$$

then the distance along the straight line between the first parallel plane and the transverse plane is

$$D_{01} = V_m (t_1 - t_0). \tag{18}$$

If the transverse plane is crossed first, then the times must be interchanged, since distances along the trajectory are taken as positive. The distance along the straight line trajectory between the transverse plane and the second parallel plane is

$$D_{12} = V_m (t_2 - t_1). \tag{19}$$

Dividing equation (18) by equation (19), and using equation (5).

$$k = \frac{D_{01}}{D_{12}} = \frac{t_1 - t_0}{t_2 - t_1} , \tag{20}$$

where k is the ratio into which the line is divided by the transverse plane. As seen from equation (20) this ratio can be determined from the times of passage of the planes by the missile. Using the lemma as given by equation (11) and the value of k as given by equation (20), it is seen that the z_1- coordinate of a point on the straight line can be determined from the times of passage of the planes. As x_1 is related to z_1 by the second of equations (2), then x_1 can also be found.

Knowing the z-coordinate of a point on the trajectory, it becomes a relative simple matter to obtain the y-coordinate. Assume that the axes of the detectors in a given plane, which are parallel to each other, make an angle ψ with the xz-plane. As seen from Figure 4,

$$y = y'' + p \tan \psi, \tag{21}$$

where y'' is the coordinate of the detector that observes the passage of the missile and p is the distance, in the plane determined by the detector axes, from the xy-plane to the point of passage. Now

$$p = \frac{z}{\cos \alpha} , \tag{22}$$

where α is the angle which the plane makes with the yz-plane. Substituting the value of p from equation (22) into equation (21),

$$y = y'' + z \frac{\tan \psi}{\cos \alpha} , \tag{23}$$

which is the y-coordinate of the position of passage of a given plane,

knowing the z-coordinate of passage and the y-coordinate of the
activated detector. Thus a point on the straight line is deter-
mined, knowing the times of passage of the planes and the position
of the activated detectors in the transverse plane.

Using the two parallel planes and the remaining transverse
plane, a second point on the trajectory is likewise determined. Thus
to determine the trajectory, it is in general, necessary and sufficient
to have at least four, noncoincident planes parallel to the y-axis of
which two are parallel to each other and the remaining two are trans-
verse, since two points are necessary and sufficient to determine the
position of a straight line.

8.3 Second Method for Determining the Trajectory

The basis of the second method for determining the target
trajectory is the relationship existing between the x- and y-coordinates
of each position of passage of the planes. In implicit form, this
relationship is

$$f_2(x,y) = x - s - (y - y'') \frac{\sin \alpha}{\tan \psi} = 0 , \tag{24}$$

which is obtained by eliminating z between equation (23) and the general
form of equations (2). The second method may be summarized in the fol-
lowing theorem:

Theorem II. A target is traversing a rectilinear trajectory
with uniform speed. The y-coordinate of the positions of the activated
detectors in the planes and the times of passage of a set of planes are
observed. All the planes of the set are parallel to the y-axis. To
determine the trajectory of the target, it is, in general, necessary and
sufficient to have the set of planes composed of at least four, non-
coincident planes for which two of the planes satisfy the condition:

$$\frac{\tan \psi_2}{\sin \alpha_2} - \frac{\tan \psi_0}{\sin \alpha_0} = 0. \tag{25}$$

The necessary and sufficient condition for theorem II as well as
lemma II is illustrated in Figure 5. As with theorem I, theorem II depends
upon a lemma which may be stated:

Lemma II. Three, noncoincident planes, parallel to the y-axis,
divide a transverse line into a given ratio. For the x- and z-coordinates
of the point of intersection of the line and one of the planes to be inde-
pendent of the x- and z-coordinates of the points of intersection of the
line and the other two planes, it is in general, necessary and sufficient
for the two planes to satisfy the condition:

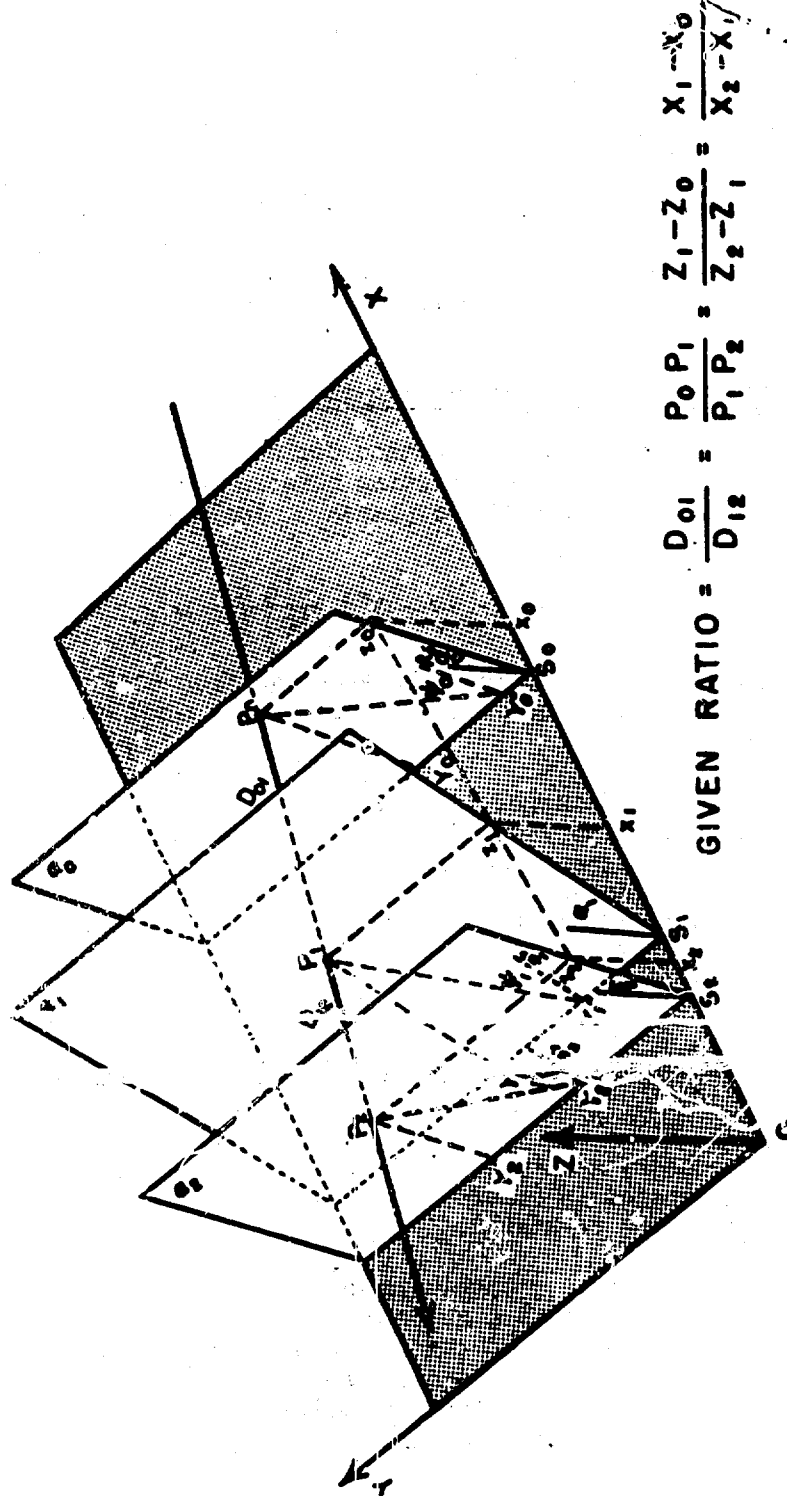$$\text{GIVEN RATIO} = \frac{D_{01}}{D_{12}} = \frac{P_0 P_1}{P_1 P_2} = \frac{Z_1 - Z_0}{Z_2 - Z_1} = \frac{X_1 - X_0}{X_2 - X_1}$$

Figure 13. Illustration of Lemmas I, II and III.

$$\frac{\tan \psi_2}{\sin \alpha_2} - \frac{\tan \psi_0}{\sin \alpha_0} = 0 \tag{26}$$

Proof of Lemma II. (Refer to Figure 13). Using the relationship between the x- and y-coordinates, equation (24),

$$f_2 (x,y) = x - s - (y - y'') \frac{\sin \alpha}{\tan \psi} = 0,$$

the first two equations of equations (1),

$$\lambda = \frac{x - x'}{D}, \quad \mu = \frac{y - y'}{D} \tag{27}$$

and proceeding as with lemma I, there is obtained

$$x_1 = \frac{y_0'' - y_1'' (1+k) + y_2'' k - s_0 \frac{\tan \psi_0}{\sin \alpha_0} + s_1 (1+k) \frac{\tan \psi_1}{\sin \alpha_1} - s_2 k \frac{\tan \psi_2}{\sin \alpha_2}}{(1+k) \left(\frac{\tan \psi_1}{\sin \alpha_1} - \frac{\tan \psi_0}{\sin \alpha_0} \right)}$$

$$+ x_2 k \frac{\frac{\tan \psi_2}{\sin \alpha_2} - \frac{\tan \psi_0}{\sin \alpha_0}}{(1+k) \left(\frac{\tan \psi_1}{\sin \alpha_1} - \frac{\tan \psi_0}{\sin \alpha_0} \right)} . \tag{28}$$

Thus it is seen, for x_1 and z_1 to be independent of x_2 and consequently z_2, that it is, in general, necessary and sufficient for

$$\frac{\tan \psi_2}{\sin \alpha_2} - \frac{\tan \psi_0}{\sin \alpha_0} = 0. \tag{29}$$

The proof of theorem II is similar to that for theorem I. By using the second equation of equations (2) with equation (28), the z_1-coordinate can be obtained. The y_1-coordinate is obtained by substituting the value of x_1 from equation (28) into equation (24). The coordinates of a second point on the line are obtained by using a fourth plane with the first and third planes.

8.3.1 Special Case for Determining the Trajectory.

When $\alpha_1 = \alpha_0$ and $s_1 \to s_0$, then $k \to 0$, giving for equation (28)

$$x_1 = s_0 + \frac{y_0'' - y_1''}{\tan \psi_1 - \tan \psi_0} \sin \alpha_0. \tag{30}$$

Substituting x_1 from equation (30) into equation (24),

$$y_1 = \frac{y_0'' - y_1''}{\tan \psi_1 - \tan \psi_0} \tan \psi_1 + y_1' \; ; \tag{31}$$

the substitution of x_1 into the second equation of equations (2) gives

$$z_1 = \frac{y_0'' - y_1''}{\tan \psi_1 - \tan \psi_\phi} \cos \alpha_0 . \tag{32}$$

Similar expressions can be written for $P_3 = (x_3, y_3, z_3)$, a second point on the trajectory.

8.4 Third Method for Determining the Trajectory.

The basis of the third method for determining the target trajectory is the relationship existing between the y- and z-coordinates of each position of passage of the planes. In implicit form, this relationship is

$$f_3 (y,z) = y - y'' - z \frac{\tan \psi}{\cos \alpha} = 0, \tag{33}$$

which is obtained by rearranging equation (23). The third method may be summarized in the following theorem:

Theorem III. A target is traversing a rectilinear trajectory with uniform speed. The y-coordinates of the positions of the activated detectors in the planes and the times of passage of a set of planes are observed. All the planes of the set are parallel to the y-axis. To determine the trajectory of the target, it is, in general, necessary and sufficient to have the set of planes composed of at least four, noncoincident planes of which two of the planes satisfy the condition:

$$\frac{\tan \psi_2}{\cos \alpha_2} - \frac{\tan \psi_0}{\cos \alpha_0} = 0. \tag{34}$$

The necessary and sufficient condition of theorem III as well as lemma III is illustrated in Figure 6. As with theorems I and II, theorem III depends upon a lemma which may be stated thus:

Lemma III. Three, noncoincident planes, parallel to the y-axis, divide a transverse line into a given ratio. For the x- and z-coordinates of the points of intersection of the line and one of the planes to be independent of the x- and z-coordinates of the points of intersection of the line and the other two planes, it is in general, necessary and sufficient for the two planes to satisfy the condition:

50

$$\frac{\tan \psi_2}{\cos \alpha_2} - \frac{\tan \psi_0}{\cos \alpha_0} = 0. \tag{35}$$

Proof of Lemma III. (Refer to Figure 13). Using the relationship between the y- and z-coordinates, equation (33)

$$f_3 (y,z) = y-y''-z \frac{\tan \psi}{\cos \alpha} = 0,$$

the second and third equations of equations (1),

$$\mu = \frac{y - y'}{D} \quad, \quad \nu = \frac{z - z'}{D} \quad, \tag{36}$$

and proceeding as with lemma I, there is obtained

$$z_1 = \frac{y_0'' - y_1'' (1+k) + k\, y_2''}{(1+k) \left(\frac{\tan \psi_1}{\cos \alpha_1} - \frac{\tan \psi_0}{\cos \alpha_0} \right)} + z_2\, k\, \frac{\frac{\tan \psi_2}{\cos \alpha_2} - \frac{\tan \psi_0}{\cos \alpha_0}}{(1+k) \left(\frac{\tan \psi_1}{\cos \alpha_1} - \frac{\tan \psi_0}{\cos \alpha_0} \right)}. \tag{37}$$

Thus it is seen for z_1 and x_1 to be independent of z_2 and consequently x_2, that it is, in general, necessary and sufficient for

$$\frac{\tan \psi_2}{\cos \alpha_2} - \frac{\tan \psi_0}{\cos \alpha_0} = 0. \tag{38}$$

The proof of theorem III is similar to that of theorem I. The x_1-coordinate is obtained by using the second equation of equations (2), and the y_1-coordinate is obtained by substituting z_1 from equation (37) into equation (33). The coordinates of a second point, $P_3 \equiv (x_3, y_3, z_3)$ are obtained by using a fourth plane with the first and second planes.

8.4.1 Special Case for Determining the Trajectory.

When $\alpha_1 = \alpha_0$ and $s_1 \rightarrow s_0$, then $k \rightarrow 0$, giving

$$z_1 = \frac{y_0'' - y_1''}{\tan \psi_1 - \tan \psi_0} \cos \alpha_0. \tag{39}$$

Substituting z_1, from equation (39), into equation (33),

$$y_1 = y_1'' + \frac{y_0'' - y_1''}{\tan \psi_1 - \tan \psi_0} \tan \psi_1 ; \tag{40}$$

SECRET

Substituting z_1 into the second of equations (2),

$$x_1 = s_0 + \frac{y_0'' - y_1''}{\tan \psi_1 - \tan \psi_0} \sin \alpha_0. \tag{41}$$

Similar expressions can be written for $P_3 = (x_3, y_3, z_3)$, a second point on the trajectory.

8.5 Comment on the Various Methods for Determining the Trajectory.

For the general case, method I requires only two rows of special detectors. By special is meant that the detectors are so designed that when one is activated its position is known; this is in addition to observing the time of activation. The other two rows of detectors need observe only the time of passage.

The special cases of methods II and III are identical. These cases require two coincident rows of special detectors for the determination of each of the two points of the trajectory. This arrangement can be simplified by designing the detectors to observe in two directions, which are the two different angles of ψ involved. By making the angles equal in magnitude, but opposite in sign, the amount of information required to be analyzed by the computer is reduced. Thus if $\psi_1 = -\psi_0$,

$$x_1 = s_0 + \frac{|y_1'' - y_0''|}{2} \frac{\sin \alpha_0}{\tan \psi_0}$$

$$y_1 = \frac{y_1'' + y_0''}{2} \tag{42}$$

$$z_1 = \frac{|y_1'' - y_0''|}{2} \frac{\cos \alpha_0}{\tan \psi_0}$$

for the first determined point P_1 on the trajectory. If $\psi_3 = -\psi_2$, then

$$x_3 = s_2 + \frac{|y_3'' + y_2''|}{2} \frac{\sin \alpha_2}{\tan \psi_2}$$

$$y_3 = \frac{y_3'' + y_2''}{2} \tag{43}$$

$$z_3 = \frac{|y_3'' - y_2''|}{2} \frac{\cos \alpha_2}{\tan \psi_2}$$

for the second determined point P_3 on the trajectory.

SECRET

AD 307724

Armed Services Technical Information Agency

ARLINGTON HALL STATION
ARLINGTON 12 VIRGINIA

FOR

MICRO-CARD

CONTROL ONLY

SECRET